2009

Spatial Detection of Multiple Movement Intentions from SAM-Filtered Single-Trial MEG for a high performance BCI

Harsha Battapady
Virginia Commonwealth University

School of Engineering
Virginia Commonwealth University

This is to certify that the thesis prepared by Harsha Battapady entitled 'SPATIAL DETECTION OF MULTIPLE MOVEMENT INTENTIONS FROM SAM-FILTERED SINGLE TRIAL MEG SIGNALS FOR A HIGH PERFORMANCE BCI' has been approved by her committee as satisfactory completion of the thesis requirement for the degree of Master of Science

Dr. Ou Bai, Director of Thesis, School of Engineering

Dr. Ding-Yu Fei, School of Engineering

Dr. Rafiq Azhar, School of Medicine

Dr. Gerald E. Miller, Chair, Department of Biomedical Engineering, School of Engineering

Dr. Rosalyn Hobson, Associate Dean, School of Engineering

Dr. Russell D. Jamison, Dean, School of Engineering

Dr. F. Douglas Boudinot, Dean of the Graduate School

Date

SPATIAL DETECTION OF MULTIPLE MOVEMENT INTENSIONS FROM SAM-FILTERED SINGLE TRIAL MAGNETO-ENCEPHALOGRAPHY SIGNALS FOR A HIGH PERFORMANCE BCI

A Thesis submitted in partial fulfillment of the requirements for the degree of Master in Sciences at Virginia Commonwealth University.

by

HARSHA BATTAPADY
Bachelor of Engineering, Mumbai University, India, 2006

Director: DR. OU BAI
ASSISTANT PROFESSOR, BIOMEDICAL ENGINEERING

Virginia Commonwealth University
Richmond, Virginia
August, 2009

Acknowledgement

I would like to thank my parents Mrs. Sharada Battapady and Mr. Narayan Battapady for believing in me. I would also like to thank my brother Mr. Vinay Battapady and Mrs. Anushree Desai for always looking out for me.

I would like to address special thanks to my advisor, Dr. Ou Bai for his personableness, support, and advice. His guidance and motivation made my Master's degree a truly successful experience. I hope he keeps supporting his students with such vigor. I also would like to thank my committee members Dr. Ding-Yu Fei and Dr. Azhar Rafiq for their insightful comments and help in completion of this work.

I would like to convey my special thanks to Ritesh Chintakuntla for his encouragement and belief in me. I would like to specially acknowledge Spandana Kankanala, Devnath Vasudevan and Lopamudra Das for always being there for me and supporting me through the good and bad times. I would like to express my gratitude to my lab mates who made working hours fun. I also would like to thank all my friends for making my stay here worthwhile.

Table of Contents

Page

List of Tables

Page

List of Figures

Page

List of Abbreviations

MEG	-	Magnetoencephalography
EEG	-	Electroencephalography
BCI	-	Brain Computer Interface
SAM	-	Synthetic Aperture Magnetometry
ERD	-	Event Related Desynchronization
ERS	-	Event Related Synchronization
GA	-	Genetic Algorithm
MLD	-	Mahalanobis linear discriminant
DTC	-	Decision Tree Classifier
SNR	-	Signal to Noise Ratio
$b_m(t)$	-	Magnetic field measured by the m^{th} detector coil
$b(t)$	-	Set of measured data
M	-	Total number of detector coils
Q	-	Total current sources assumed to generate neuromagnetic field
r	-	Location of sources
T	-	Matrix transpose
R_b	-	Covariance matrix
R_s	-	Covariance matrix of the source-moment activity

$s(t)$	-	Source magnitude vector
$l(r)$	-	Lead-field vector in the source-moment direction
$L(r)$	-	Lead field vector
L_c	-	Composite lead field matrix
ζ	-	Direction
$l_m^{\zeta}(r)$	-	m^{th} sensor o/p induced by unit magnitude source located at r and ζ direction
$\eta(r_q, t)$	-	Orientation of the q^{th} source in 3D column vector
ψ	-	Orientation of all Q sources
$n(t)$	-	Additive noise
$w(r)$	-	Column vector for filter weight
$w_m(r)$	-	Weight vector for minimum variance beamformer
I	-	Unit matrix
σ^2	-	Variance
RMC	-	Right Motor Cortex
LMC	-	Left Motor Cortex
VC	-	Virtual channel

Abstract

SPATIAL DETECTION OF MULTIPLE MOVEMENT INTENSIONS FROM SAM-FILTERED SINGLE TRIAL MEG SIGNALS FOR A HIGH PERFORMANCE BCI

By Harsha Battapady, M.S.

A Thesis submitted in partial fulfillment of the requirements for the degree of Master in Sciences at Virginia Commonwealth University.

Virginia Commonwealth University, 2009

Major Director: Dr. Ou Bai
Assistant Professor, Dept. of Biomedical Engineering

The objective of this study is to test whether human intentions to sustain or cease movements in right and left hands can be decoded reliably from spatially filtered single trial magneto-encephalographic (MEG) signals. This study was performed using motor execution and motor imagery movements to achieve a potential high performance Brain-Computer interface (BCI). Seven healthy volunteers, naïve to BCI technology, participated in this study. Signals were recorded from 275-channel MEG and synthetic aperture

magnetometry (SAM) was employed as the spatial filter. The four-class classification for natural movement intentions was performed offline; Genetic Algorithm based Mahalanobis Linear Distance (GA-MLD) and direct-decision tree classifier (DTC) techniques were adopted for the classification through 10-fold cross-validation. Through SAM imaging, strong and distinct event related desynchronisation (ERD) associated with sustaining, and event related synchronisation (ERS) patterns associated with ceasing of hand movements were observed in the beta band (15 - 30 Hz). The right and left hand ERD/ERS patterns were observed on the contralateral hemispheres for motor execution and motor imagery sessions. Virtual channels were selected from these cortical areas of high activity to correspond with the motor tasks as per the paradigm of the study. Through a statistical comparison between SAM-filtered virtual channels from single trial MEG signals and basic MEG sensors, it was found that SAM-filtered virtual channels significantly increased the classification accuracy for motor execution (GA-MLD: 96.51 ± 2.43 %) as well as motor imagery sessions (GA-MLD: 89.69 ± 3.34%). Thus, multiple movement intentions can be reliably detected from SAM-based spatially-filtered single trial MEG signals. MEG signals associated with natural motor behavior may be utilized for a reliable high-performance brain-computer interface (BCI) and may reduce long-term training compared with conventional BCI methods using rhythm control. This may prove tremendously helpful for patients suffering from various movement disorders to improve their quality of life.

CHAPTER 1

Introduction

1.1. Literature Review:

1.1.1. *Need for BCI:*

Patients with degenerative diseases such as amyotrophic lateral sclerosis (ALS), muscular dystrophy and multiple sclerosis or from traumatic brain or spinal cord injury all suffer from the inability to control voluntary muscle movements. Without voluntary muscle control, these patients are unable to effectively communicate their needs to the environment. In the later stages of such diseases, though their cognitive ability remains intact, they may become completely trapped in their own body or "locked-in". Brain-Computer Interfaces (BCIs) may provide an effective solution for patients with such diseases to improve their quality of life. BCIs are devices that allow for communicating intentions for gross motor control by analyzing brain activity and not the muscle movements (Wolpaw et al. 2002). The development of BCI technology thus proves to be immensely advantageous to patients in the 'locked-in' or semi- 'locked-in' stage, where

BCI can be used as a communication and rehabilitation tool. Direct brain communication or control may offer patients a possible way to interact with the external world.

BCIs can be used for decoding brain signals and control applications based on brain signals invasively or non-invasively. A highly reliable and fast BCI for multi-dimensional control can be achieved using invasive methods, but they have inherent technical difficulties such as the need for chronic implantable recording and risks due to surgical implantation of electrodes. Due to such difficulties non-invasive methods are generally used. Electro-encephalogram (EEG) and Magneto-encephalogram (MEG) have emerged as viable noninvasive options. Both have time resolutions in milliseconds so we can study the dynamic activities within specific cortical regions of the brain in contrast to imaging-based BCI (Laconte et al. 2006). For the present study, the advantages of MEG were explored to propose a high performance BCI.

1.1.2. *Magneto-encephalography (MEG)*

MEG is a discipline that deals with detection and interpretation of magnetic fields produced by the human brain. MEG measurements span a frequency range from about 10 mHz to 1 kHz (or perhaps as low as 1 mHz for sleep studies) and field magnitudes from about 10 fT for spinal cord signals to about several picotesla for brain rhythms (Nakaya and Mori 1992). MEG signals can be affected by the Earth's field magnitude, which is about 0.5 mT and the urban magnetic noise which is about 1 nT to 1 μT, i.e. a factor of 1

million to 1 billion larger than the MEG signals. Such large differences between signal and noise demand noise cancellation with extraordinary accuracy.

MEG signals are measured on the surface of the head and they reflect the current flow in the functioning brain. The cortex (see Fig. 1a) contains well-aligned pyramidal cells, which consist of dendrites, cell body, and axon and there are approximately 10^5 to 10^6 cells in area of about 10 mm^2 of cortex (Carpenter 1985). There are many connections between various parts of the brain mediated by nerve fibers which are connected to dendrites and cell bodies of other nerve cells via synapses. In the whole brain there are approximately 10^{10} cells and about 10^{14} synaptic connections.

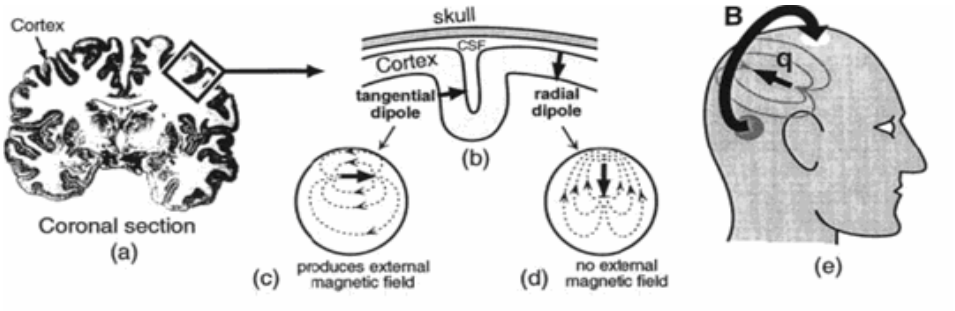

Figure 1: Origin of the MEG signal (Vrba and Robinson 2001).(a) Coronal section of the human brain. Cortex is indicated by dark color. The primary currents flow roughly perpendicular to the cortex. (b) The cortex has numerous sulci and gyri and its convoluted nature gives rise to the currents flowing either tangentially or radially relative to the head. The head can be approximated by a spherical conducting medium. (c) Tangential currents will produce magnetic fields that are observable outside the head. (d) Radial currents will not produce magnetic fields outside the head. (e) Magnetic fields due to cortical sources will exit and re-enter the scalp.

Because of ionic exchange between the cell and its surroundings, the equilibrium between diffusion processes and electrical forces establishes negative potentials of about -70 mV within the cell (Partridge 1993). Cell stimulation (chemical, electrical, or even mechanical) can cause alteration of the cell's trans-membrane potential and can lead to cell depolarization (or hyper-polarization). Such changes can occur, e.g., at the synapse, when neurotransmitters are released. Because the cell is conductive, the depolarization (or hyper-polarization) causes current flow within the cell (called the impressed or intracellular current) and a return current outside the cell (called volume or extra-cellular current).

The dendritic current due to cell depolarization (or hyper-polarization) flows roughly perpendicular to the cortex. However, the cortex is convoluted with numerous sulci and gyri and, depending on where the cell stimulation occurred; the current flow can be either tangential or radial to the scalp surface (See Fig. 1b) If the brain could be modeled as a uniform conducting sphere, then due to symmetry, only the tangential currents would produce fields outside the sphere (Sarvas 1987) (See Figs. 1c and e) and the radial currents would produce no magnetic fields (See Fig. 1d). If the magnetic detectors were radial to the head, then MEG would be mostly sensitive to the impressed intracellular currents, while EEG would detect the return volume currents.

Current flow within a single cell is too small and cannot produce observable magnetic fields outside the scalp. For fields to be detectable, it is necessary to have nearly simultaneous activation of a large number of cells, typically 10^4 to 10^5 (Wikswo 1989). Generally, the MEG sources are distributed; however, activation of even large numbers of

cells can often be assumed spatially small and can be modeled by a point equivalent current dipole (Williamson and Kaufman 1981).

MEG measures the distribution of magnetic fields on the two-dimensional head surface. However, the required information is usually a three-dimensional distribution of currents within the brain. Unfortunately the field inversion problem is non-unique and MEG data must be supplemented by additional information, physiological constraints, or mathematical simplifications. One way to supply more information is to also use EEG. Both MEG and EEG measure the same sources of neuronal activity and their information is complementary (Vieth et al. 1995). Additional information to assist field inversion can also be supplied by other imaging techniques. For structural information one can use magnetic resonance imaging (MRI) and computed axial tomography (CAT) and for functional information one can use positron emission tomography (PET), single photon emission computed tomography (SPECT), and functional MRI (fMRI). (Vrba and Robinson 2001)

MEG Set-up: A typical MEG system is a complex installation as shown in the schematic diagram in Fig. 2. The Superconducting Quantum Interference Devices (SQUID) detectors of magnetic field are housed in a cryogenic container called a dewar, which is usually mounted on a movable gantry for horizontal or seated positions. SQUID detectors are very sensitive magnetometers used to measure very small magnetic fields, based on superconducting loops containing Josephson junctions(Josephson 1974). The subject or patient is positioned on an adjustable bed chair. The SQUID system and patient may or

may not be positioned in a shielded room. At present, the majority of installations use shielded rooms; however, progress is being made toward unshielded operations. The MEG measurement is usually supplemented by EEG and both MEG and EEG signals are transmitted from the shielded room to the SQUID and processing electronics and the computers for data analysis and archiving. The MEG system also contains stimulus delivery and its associated computer, which is synchronized with the data acquisition. The installation is completed with a video camera(s) and intercom for observation of and communication with the subject in the shielded room. (Vrba and Robinson 2001)

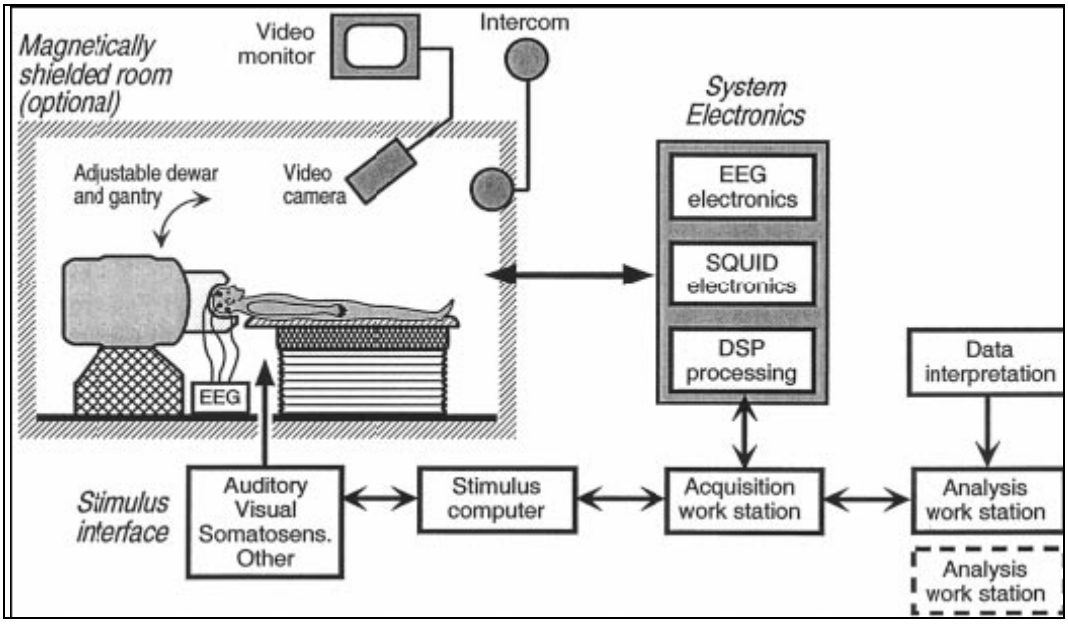

Figure 2: Schematic diagram of an MEG installation

(http://strategis.ic.gc.ca/pics/ht/ctfsystems.html)

1.1.3. *MEG vs. EEG:*

Human natural voluntary movement can be associated with frequency changes occurring in the alpha (8-14 Hz) and beta (15-30 Hz) bands. There are two distinct power changes seen in EEG in both alpha and beta bands, the event-related desynchronization (ERD) or power decrease that occurs up to 2 s before movement and is sustained with continuous movement (Toro et al. 1994; Bai et al. 2005) and the event-related synchronization (ERS) or power increase, usual only seen in beta band, occurring after the end of movement (Pfurtscheller 1988). The beta frequency band has been implicated as important in various motor control processes including sensorimotor integration and motor learning (Andres and Gerloff 1999). According to human somatotopic studies, human limbs are controlled by contra-lateral sensorimotor areas of the brain hemispheres. Right and left hand movements activate contra-lateral motor areas in the brain. However, the source localization of ERD/ERS with EEG is poor due to limited spatial resolution. This is partially due to the return volume currents generated due to the convolution of the cortex by numerous sulci and gyri (Vrba and Robinson 2001). MEG measures the magnetic fields produced by the electrical activity in the brain. It provides direct information about the dynamics of evoked and spontaneous neural activity via the extremely sensitive super conducting quantum interference devices (SQUIDs). It is least affected by the spatial blurring effects of the skull (Salmelin et al. 1995) produced by the return volume currents and thus obtains a better signal to noise ratio (SNR) as compared to EEG. Particularly for single trial studies, MEG can prove very advantageous due to the high SNR property and

consequently its ability for source localization. Accordingly, it is superior in studies related to movement related beta-ERD/ERS recordings.

1.1.4. *Limitations of MEG*

MEG has many benefits namely it is completely noninvasive and non-hazardous. The data can be collected in the natural seated position allowing more life-like cognitive experiments. MEG has an extremely high temporal resolution (milliseconds) and also provides a good spatial resolution. Signals can be recorded over the whole cortex. There is no need to paste electrodes on the scalp as with EEG.

However, a major technical problem associated with MEG is that the localization of sources of electrical activity within the brain from magnetic measurement outside the head is complicated and does not have a unique solution. This is known as the ill-posed inverse problem, and is itself the subject of research. However, as indicated above, feasible solutions can be often obtained by using relatively simple models.

Due to the increased distance to sources and the almost spherical symmetry of the head it is difficult to provide reliable information about subcortical sources of brain activity. MEG does not provide structural/anatomical information. Therefore MEG data often must be combined with MR data into a composite image of function overlaid on anatomy to produce activation maps. We used Synthetic Aperture Magnetometry (SAM) to achieve this.

1.2. *Synthetic Aperture Magnetometry (SAM)*

Previously, most MEG data analysis focused on the average evoked potential paradigm (Hillebrand et al. 2005). However, with the advent of large MEG sensor arrays with whole-head coverage, it was found that the evoked response mapped by a large whole-head array was almost identical to that detected by serial multiple placement and measurement by single-channel MEG sensor at the same sites. Signal averaging did not make use of information available from large MEG sensor arrays. In contrast to this, the unaveraged or single-trial MEG signals seemed to exhibit spatial and temporal correlations which could be used for better signal to noise ratio (SNR) and source localization of the activity (Vrba and Robinson 2001). Synthetic Aperture Magnetometry (SAM) is a novel spatial filtering technique which achieves three-dimensional source estimation during task performance (Robinson 1998). It uses the spatial and temporal correlation of the MEG sensor array. It is based on the nonlinear constrained minimum variance beamformer. It thus provides excellent spatial resolution and can image a high signal-to-noise ratio (SNR) of the unaveraged or single-trial MEG signals.

1.2.1. *Minimum variance beamformer*

The minimum variance beamformer has been one of the most popular spatial-filter techniques in various signal-processing fields. It has also been applied to neuromagnetic

source localization(Spencer et al. 1992; vanDrongelen et al. 1996; VanVeen et al. 1997; Robinson and Vrba 1999). Synthetic Aperture Magnetometry (SAM) is based on this method.

Let the magnetic field measured by the mth detector coil at time t be $\mathbf{b}_m(t)$, and a column vector $\boldsymbol{b}(t) = [b_1(t), b_2(t),\ldots, b_M(t)]^T$ be a set of measured data where M is the total number of detector coils and the superscript T indicates the matrix transpose. A spatial location is represented by a 3D vector $\boldsymbol{r}$: $\boldsymbol{r} = (x, y, z)$. A total of Q current sources are assumed to generate the neuromagnetic field, and the locations of these sources are denoted as $\boldsymbol{r}_1, \boldsymbol{r}_2 \ldots \boldsymbol{r}_Q$. The moment magnitude of the qth source at time t is denoted as $s(\boldsymbol{r}_q, t)$, and the source magnitude vector is defined as $\boldsymbol{s}(t) = [s(\boldsymbol{r}_1, t), s(\boldsymbol{r}_2, t)\ldots, s(\boldsymbol{r}_Q, t)]^T$. The orientation of the qth source is defined as a 3D column vector $\eta(\boldsymbol{r}_q, t) = [\eta_x(\boldsymbol{r}_q, t), \eta_y(\boldsymbol{r}_q, t), \eta_z(\boldsymbol{r}_q, t)]^T$ whose ψ component (where ζ equals x, y, or z in this study) is equal to the cosine of the angle between the direction of the source moment and the ζ direction. We assume that the orientation of each source is time independent. Omitting the time notation t, we define a $3Q$ X Q matrix that expresses the orientations of all Q sources as $\boldsymbol{\psi}$ such that

$$\boldsymbol{\psi} = \begin{bmatrix} \eta(r_1) & 0 & \cdots & 0 \\ 0 & \eta(r_2) & 0 & \vdots \\ \vdots & 0 & \ddots & 0 \\ 0 & \cdots & 0 & \eta(r_Q) \end{bmatrix}$$

Let $l_m^{\zeta}(\boldsymbol{r})$ be the mth sensor output induced by the unit-magnitude source located at $\boldsymbol{r}$ and directed in the ζ direction. The column vector $\boldsymbol{l}_{\zeta}(\boldsymbol{r})$ is defined as $l_{\zeta}(\boldsymbol{r}) = [l_1^{\zeta}(\boldsymbol{r}), l_2^{\zeta}(\boldsymbol{r}), \ldots, l_M^{\zeta}(\boldsymbol{r})]^T$. The lead field matrix, which represents the sensitivity of the whole sensor array at

$\boldsymbol{r}$, is defined as $\boldsymbol{L}(\boldsymbol{r}) = [\boldsymbol{l}_x(\boldsymbol{r}), \boldsymbol{l}_y(\boldsymbol{r}), \boldsymbol{l}_z(\boldsymbol{r})]$. For later use, the lead-field vector in the source-moment direction is defined as $\boldsymbol{l}(\boldsymbol{r})$; it is obtained by using $\boldsymbol{l}(\boldsymbol{r}) = \boldsymbol{L}(\boldsymbol{r})\ \eta(\boldsymbol{r})$. The composite lead field matrix for the entire set of Q sources is defined as

$$L_c = \left[L(r_1), L(r_{21}), \cdots, L(r_1)\right]$$

The relationship between $\boldsymbol{b}(t)$ and $\boldsymbol{s}(t)$ is then expressed as

$$b(t) = \left(L_c \boldsymbol{\psi}\right) s(t) + n(t),$$

where $\boldsymbol{n}(t)$ is the additive noise.

Let the measurement covariance matrix be $\boldsymbol{R}_b$; i.e., $\boldsymbol{R}_b = \left\langle b(t) b^T(t) \right\rangle$, where $\langle \cdot \rangle$ indicates the ensemble average (this ensemble average is usually replaced with the time average over a certain time window). Let the covariance matrix of the source-moment activity be $\boldsymbol{R}_s$; i.e., $\boldsymbol{R}_s = \langle \boldsymbol{s}\ (t)\ \boldsymbol{s}^{\boldsymbol{T}}(t) \rangle$. Then, the relationship between the measurement covariance matrix and the source-activity covariance matrix is such that;

$$R_b = \left(L_c \boldsymbol{\psi}\right) R_s \left(\boldsymbol{\psi}^T L_c^T\right) + \sigma^2 I\ ,$$

where the noise in the measured data is assumed to be the white Gaussian noise with the variance of σ^2 and $\boldsymbol{I}$ is the unit matrix.

To estimate the source moment, a class of techniques referred to as the spatial filter was used. The spatial filter techniques use the following simple linear operation for estimating the source moment,

$$\hat{s}(r,t) = w^T(r) b(t)\ ,$$

where $s\hat{}(\boldsymbol{r}, t)$ is the estimated magnitude of the source moment at $\boldsymbol{r}$ and time t. In this equation, $\boldsymbol{w}(\boldsymbol{r})$ is a column vector characterizing the filter weight. Note that because this

weight vector is calculated for any spatial location $\boldsymbol{r}$, the source-moment distribution can be reconstructed by scanning the output of the spatial filter over a region of interest in a perfectly post-processing manner. One well-known spatial filter of this kind is the minimum-variance distortion-less beamformer originally developed for seismic-array signal processing (Capon 1969). In this technique, the filter weight vector $\boldsymbol{w}_m(\boldsymbol{r})$ is obtained by minimizing $w_m^T(r)\, R_b\, w_m(r)$ under the constraint of $l^T(r) w_m(r) = 1$. The explicit form of the weight vector for the minimum- variance beamformer is known to be

$$w_m(r) = \frac{R_b^{-1} l(r)}{l^T R_b^{-1} l(r)}$$

In the present study, we employed SAM as a spatial filter for single trial MEG signals to design a BCI that classifies human movement intention to sustain right/left hand motor execution or motor imagery featured by ERD or to cease right/left hand motor execution or motor imagery featured by ERS. The results were compared to MEG sensor based classification to verify the effectiveness of SAM. We hypothesized that the SAM-filtered MEG signal would provide better signal to noise ratio and facilitate a fast and reliable detection/classification of motor activities, eventually leading to a high performance BCI.

CHAPTER 2

Methods

2.1. Subjects

Seven healthy volunteers, 5 male and 2 female (age: 31±8 years) participated in the experiment. All subjects participating in this study were naïve to BCI and right-handed according to the Edinburgh inventory (Oldfield 1971). The protocol was approved by the Institutional Review Board. All subjects gave written informed consent for the study.

2.2. Experimental paradigm

A visual instruction cue randomly selected from a set of four cues: RYES, LYES, RNO and LNO was presented on a computer screen placed about 50cm before the subject (Fig. 3, Pg. 17). The subjects were instructed to perform either physical or imaginary movements of their right or left hand after the initial cue presentation depending on the type of trial. They had to begin with or imagine repetitive wrist extensions of the right or

left arm at the onset of the initial cue RYES, RNO, LYES or LNO. After 2.5sec a RESPONSE cue was displayed at which time the subject, depending on the YES or NO cue for the right/left hand had to sustain (ERD) or cease (ERS) the hand movements respectively.

At 4 s, a STOP cue was given, the response cue disappeared, after which the subject had to cease all movements and return to baseline rest. A 6 s ~ 7 s rest period was given after which the process was repeated. During the period of visual stimuli the subjects were asked to keep eyes open and reduce blinks as much as possible. The subjects were allowed to become familiar with the paradigm before data recording. Subjects were asked to keep the head still during recording to reduce head motion.

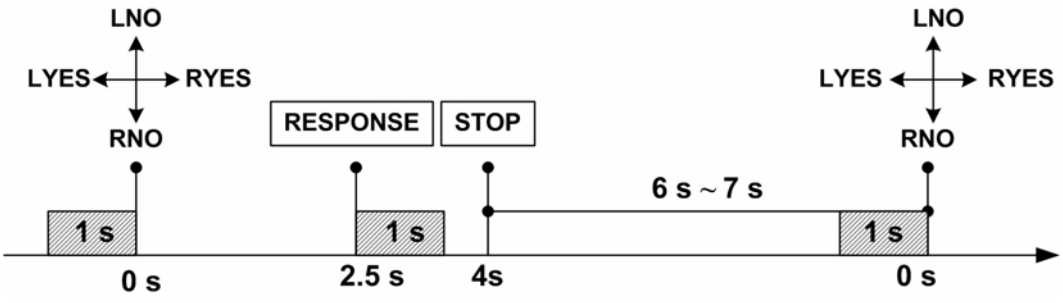

Figure 3: Experimental paradigm: Activation period: 0s to 1s after RESPONSE cue, i.e. 2.5s – 3.5s. Control period: -1s to 0s before the initial warning cue of Right Yes RYES, Left Yes LYES, Right No RNO or Left No LNO. The subjects began repeated wrist extensions of either the right or left hand as per the initial warning cue. At the RESPONSE cue, for RYES/ LYES, the subjects continued wrist extensions, for RNO/ LNO the wrist extensions were ceased till the STOP cue. From the STOP cue, there was a rest period of 6 s ~ 7 s. Data from the activation and control windows were used for SAM analysis, with virtual channels during the activation period with respect to the control period used for classification/prediction. Initial warning cue (RYES, RNO, LYES, or LNO) period: 0s - 2.5s, RESPONSE cue period: 2.5s – 4s, STOP (Rest) cue period: 6 s ~ 7 s. The same paradigm was used for motor execution and motor imagery.

2.3. Data Acquisition

MEG data was recorded at sampling frequency of 600 Hz using a 275-channel CTF whole head MEG system (VSM MedTech Inc., Coquitlam BC, Canada) in a shielded environment. The CTF MEG system is equipped with synthetic 3rd gradient balancing, an active noise cancellation technique that uses a set of reference channels to subtract background interference.

High-resolution structural MRI images were also acquired for co-registration for each subject using a magnetization-prepared rapid acquisition by gradient echo sequence (MP-RAGE) (TI/TE/TR/FA=725/2.928/7.6/6°, FOV=22 cm, partition thickness=1.2mm, 256 x 256, in-plane voxel size=0.859375).

EMG was recorded using bipolar electrodes over the right and left wrist extensors. This allowed for the exclusion of any trial, not following the experimental paradigm for actual right/left hand movements and also the exclusion of any trial with movement prior to the warning cue by monitoring for premature muscular activity. For subject S 7, the motor execution session contained excessive movement artifacts and was excluded due to these performance glitches during data recording. The motor imagery session for subjects S 2 and S 6, was excluded from the analyses due to the lack of number of samples in individual events (RYES, RNO LYES, and LNO). Subject S1 did not participate in the motor imagery session.

2.4. SAM Analysis

Synthetic Aperture Magnetometry (SAM) was used for source localization of MEG signals. “Source localization” implies simplification of the complex activity of a very large numbers of neurons to a few parameters that help describe that activity (Robinson 2004). SAM is a minimum variance beamformer technique. A beamformer is designed to pass the signal from a small region of interest with unit gain while blocking signals from outside that area (Keefer et al. 2008). Thus, the small area signal would be an estimate of the activity in that area. SAM has thus been used to image source power or source signal-to-noise ratio from MEG (Robinson 2004). It characterizes the spatial distribution of event-related changes in cortical rhythm within a specified frequency range and time window, relative to the events (Robinson 2004).

2.4.1. SAM Imaging

MEG analysis software developed at National Institute of Mental Health (NIMH) MEG core facility was used for epoching data, SAM analysis and MRI conversion. For all measurements, fiducial skin markers were placed on subjects' nasion and bilateral preauricular points.

The data was epoched according to the marker events for a period of 9 sec starting 1 sec before the instruction cue and continuing 8 sec after. For SAM analysis, all epoched data for each task (RYES, RNO, LYES, or LNO) were combined together to form a grand dataset. Before SAM analysis, a multisphere head model was created for each subject (threshold value ≈ 40%) based on anatomical images of each subject using MEG analysis software.

For SAM Analysis, single-trial event-related MEG data from the grand datasets were used to compute covariance matrices for each dataset corresponding to each task (RYES, RNO, LYES, and LNO). The frequency range of interest was the beta band i.e. 15-30 Hz. For Physical movements (see Fig. 3), the active state was defined between the RESPONSE cue to 1 sec after cue onset (2.5s – 3.5s) and -1s to movement onset (instruction cue) was set as the control state (-1s – 0s). For Imaginary movements, the response of the subjects to RESPONSE cue was delayed and hence, a 0.5 sec delay was introduced for the active state (3s – 4s, see Fig. 3), the control state (-1s – 0s, see Fig. 3) remained unchanged. These parameters were fed in to compute the covariance between the active and the control states. For ERD/ERS analysis a statistical parametric image was

computed, on a voxel- by-voxel basis, from the difference in cortical power for the two states, relative to their noise variance. Only voxels displaying statistically significant power changes were displayed in color scale on the individual MRI. Thus an optimal spatial filter was designed which created a 3D source image comparing the source strength for the two states. This image was superposed on the MRI image of the subjects to obtain the source- signal-to-noise ratio image corresponding to each event for all the subjects. To get an impression of how the 3-D images look like, an example of ERD/ ERS tasks is shown in Fig. 4.

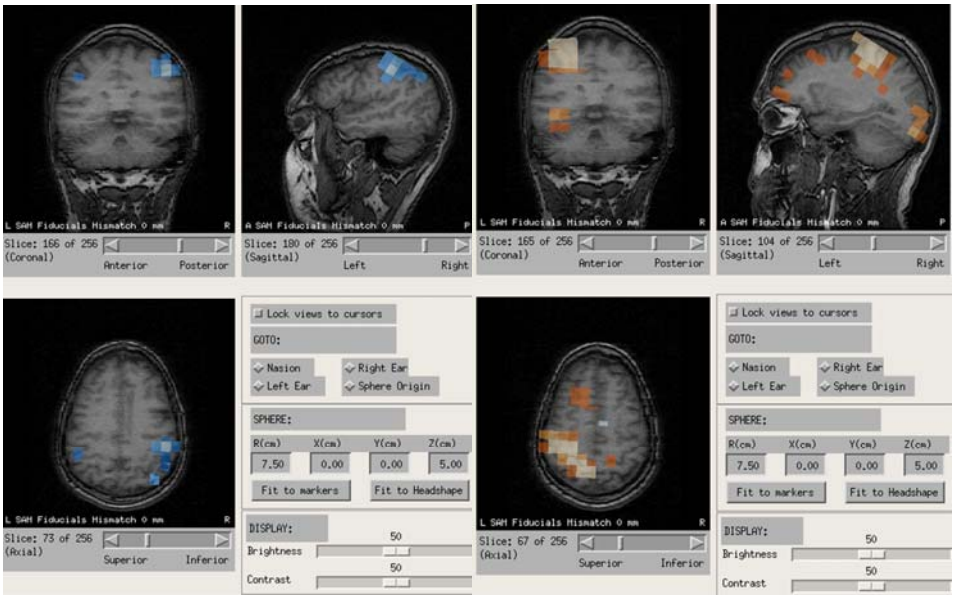

Figure 4: 3-D SAM images. Coronal, Sagittal and Axial view of the human brain corresponding to ERD (blue)/ ERS (red) tasks for the upper limb movements.

2.4.2. Virtual channel selection

A *virtual channel* is similar to a regular MEG channel, except that it is tuned to a particular source or target. For regular SAM analysis as described above, a beamformer is calculated for each voxel of the image, and the beamformer is used to calculate a source power estimate. To calculate the virtual channel, the same beamformer was used, but in a different way. A beamformer is just a set of coefficients, or weights, one for each channel, and a virtual channel is just a weighted sum of all the MEG channels with those weights (http://kurage.nimh.nih.gov/meglab/Meg/Meg).

The target location for the present study was the motor cortex area. As previously described, human limb movements are controlled by contalateral sensorimotor areas. It was of interest to study the activity associated with right and left hand movements in the beta band. The source-signal-to-noise ratio image obtained through SAM analysis had high activity regions in these areas. For the right and left hand physical movements as well as motor imagery, for the YES (sustain movement) case, virtual channels were selected from regions showing strong ERD in the left and right motor cortex area respectively (See Fig. 6, Pg. 33). Similarly for the right and left hand physical movements as well as motor imagery, for the NO (cease movement) case, virtual channels were selected from regions showing strong ERS in the left and right motor cortex area respectively (See Fig. 6, Pg. 33). Around 20-30 virtual channels were selected for each subject.

2.5. Time-course Analysis of MEG Sensor and Virtual channel Data

The digital MEG signal was sent to a DELL PC workstation and was offline processed using a home-made MATLAB (Math Works, Natick, MA) Toolbox: brain-computer interface to virtual reality or BCI2VR (Bai et al. 2007; Bai et al. 2008). This was used for time-course analysis, feature extraction and classification for MEG-Sensor domain as well as Virtual channel data.

2.5.1. Time-Frequency Analysis of MEG Sensor Data

Time-Frequency analysis was performed on the MEG sensor data (See Fig. 7, Pg. 44) to observe the power (ERD/ERS) patterns for each event (RYES, RNO, LYES, and LNO). Since it was intended to study movement intention associated cortical activities, the region of interest for the present study was assumed to be the motor cortex area (Pfurtscheller and Berghold 1989a; Toro et al. 1994; Pfurtscheller and Lopes da Silva 1999). The MEG channels constrained to the central MEG sensors (See Fig. 5) associated with the right or left motor cortex area were used for the analysis. It was intended to analyze the power in the beta band, i.e. the ERD/ERS patterns with respect to the time-course of the motor execution as well as motor imagery tasks.

Power in the frequency range 0- 60 Hz, for right and left hand movements was calculated using Welch method, which was applied with the use of a Hamming window to reduce side-lobe effect and estimation variance (Welch 1967). A baseline correction was

introduced from -1 s to 0 s. The length of the sliding window was 1 s with a slide increment of 0.1 s. The segment length was 0.25 s with frequency resolution of 4 Hz and there was no overlapping between consecutive segments.

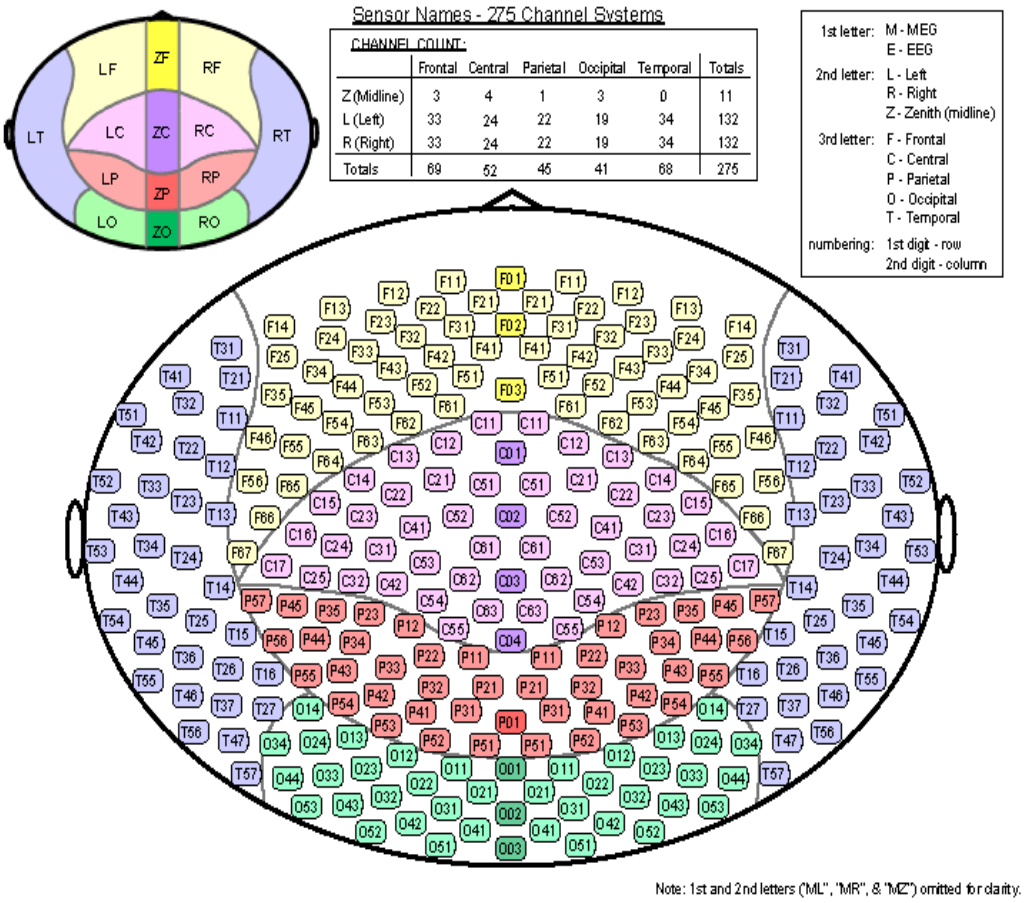

Figure 5: MEG- 275 channel system
(http://kurage.nimh.nih.gov/library/Meg/SensLayout-275.pdf)

2.5.2. Time-course of Event-related Power for Virtual channel Data

An event related power analysis was performed on the virtual channels obtained through SAM analysis (See Fig. 8, Pg. 37) to observe the ERD/ERS patterns over these channels, for each event (RYES, RNO, LYES, and LNO) with respect to the parameters of the present study. The time-course of event-related power was obtained from the variance of virtual channel signal in a sliding window with length of 1s and a slide increment of 0.1 s. These virtual channels were already filtered from the beta band. A baseline correction was introduced from -1 s to 0.5 s.

Event related power analysis was mainly done to verify whether, ERD was a dominant pattern for virtual channels selected from the sustaining movement related events (RYES, LYES) and whether ERS was dominant for virtual channels selected from the ceasing of movement related events (RNO, LNO). This was performed for both physical and motor imagery virtual channel data.

2.6. Feature Extraction and Classification

2.6.1. Feature extraction for MEG sensors and Virtual channels

For SAM-filtered virtual channel based classification of movement intensions from MEG data, the channel reduction was achieved through selection of virtual channels. Similarly, for MEG -Sensor based classification, the MEG channels were constrained through empirical channel reduction; this covered the entire motor cortex area. Thus central 52 MEG channels were used for sensor based classification. (See Fig. 5). Also, the selection of beta band (15- 30 Hz) to study ERD/ERS served as an important parameter for feature reduction. In the MEG-Sensor domain, the power samples were calculated in the beta band (15- 30 Hz) for the active state period during motor execution (2.5 s – 3.5 s) and motor imagery (3 s – 4 s), the segment length was 0.25 s with no overlapping between consecutive segments. For Virtual channels, the beta band power samples were created from the active state period, which was different for motor execution (2.5 s – 3.5 s) and motor imagery (3 s – 4 s) events, as the variance of the data samples for the tasks RYES, RNO, LYES and LNO.

2.6.2. Feature Selection and Classification

Feature Selection

Bhattacharyya distance: The Bhattacharyya distance is the square of mean difference between two task conditions divided by the averaged variance of the samples in two task conditions so that a larger Bhattacharyya distance will lead to better classification accuracy (Marques 2001). Bhattacharya distance was applied to the feature selection for the classification from SAM-filtered virtual channel signals and MEG Sensor signals. The feature with the largest Bhattacharyya distance was selected for the classification of 'Yes' and 'No' intentions of both right and left hand physical movements and motor imagery.

Genetic Algorithm (GA): Genetic algorithms are computational models inspired by evolution (Whitley 1994). As such, they encode a potential solution as a chromosome-like data structure and apply recombination operators on these structures (Yom-Tov and Inbar 2002). In this case, the chromosomes are combinations of a predetermined number of features selected from SAM-filtered virtual channel signals and MEG sensor signals.

Classification

The signals from the specified single-trial MEG, virtual channel and the sensor domain data were fed into classification techniques developed in home-made MATLAB (Math Works, Natick, MA) Toolbox: brain-computer interface to virtual reality or

BCI2VR (Bai et al. 2007; Bai et al. 2008) based on movement related signals. It was intended to use these classification techniques to reliably decode movement intentions spatially for the proposed high performance BCI. 10-fold cross-validation (90% training set, 10% testing set) technique was adopted for classification. It was intended to discriminate four movement intentions (RYES, RNO, LYES and LNO) while sustaining and ceasing the movement from single trial MEG signals. The techniques used were as follows:

GA-based Mahalanobis Linear Distance Classifier (GA-MLD): The Mahalanobis Distance Classifier had proved effective for classification in previous studies (Babiloni et al. 2001; Bai et al. 2007), it was further optimized using GA-based feature extraction method. The optimal feature subset was selected by GA, and the selected features providing the best cross-validation accuracy were applied to a Mahalanobis Linear Distance Classifier. Mahalanobis linear distance was measured, which computed a pooled covariance matrix averaged from individual covariance matrices in all task conditions where the discriminant boundaries were hyper-planes leaning along the regressions (Marques 2001). The number of features for the subset was 4, which was determined from the 10-fold cross-validation accuracy with feature numbers of 2, 4, 6, and 8.

Direct Decision Tree Classifier (DTC): Decision tree is a classifier which uses symbolic treelike representations of finite sets of if-then-else questions that are natural, intuitive and interpretable (Duda et al. 2001). A certain feature subset, for example, channels over left motor cortex area are associated with right hand movement (Kawashima et al. 1993;

Volkmann et al. 1998; Jung et al. 2003) and hence would be the best to discriminate intention to move the right hand, whereas operate rather poorly for the discrimination of other movement intentions. We used multistage classification, i.e., decision tree classifier (DTC), to discriminate one intention from others in each successive stage. At each level of DTC, the features for one-to-others classification were ranked by Bhattacharya distance (see detail method in (Bai et al. 2007)) and the 4 features with higher rank were used for classification by MLD. The number of the feature for classification was determined from preliminary comparison with numbers of 2, 4, 6 and 8.

CHAPTER 3

Results

3.1. Neurophysiological analysis of ERD and ERS in SAM domain

The proposed BCI in this study intended to discriminate the ERD, associated with sustained motor execution or motor imagery, from ERS associated with ceasing motor execution or motor imagery in the beta band from single trial MEG signals. To give an impression of SAM images and virtual channel selection, the source-signal-to-noise images obtained from SAM analysis are shown in Fig. 6. Data from the active and control states were used for the analysis. The control state used was between -1 s – 0 s. The regions of high activity, displaying ERD and ERS for motor execution tasks were clearly seen for the active state between 2.5 s to 3.5 s. For motor imagery, regions of high activity were observed for the active state between 3 s to 4 s. This was due to the subjects' delayed response to visual cues (RYES, RNO, LYES an LNO) during the motor imagery tasks. Virtual channels were selected from the regions of high activity, for power analysis, feature extraction and classification. From the SAM images obtained for both motor

execution and motor imagery, it was observed that ERD/ERS signals were more enhanced during motor execution than for motor imagery.

Hemispheric asymmetry which suggests that the contra-lateral hemisphere is predominantly involved with dominant hand movement, whereas both contra-lateral and ipsilateral hemispheres are involved with non-dominant hand movement was also established from the SAM images (Kawashima et al. 1993; Volkmann et al. 1998; Jung et al. 2003).

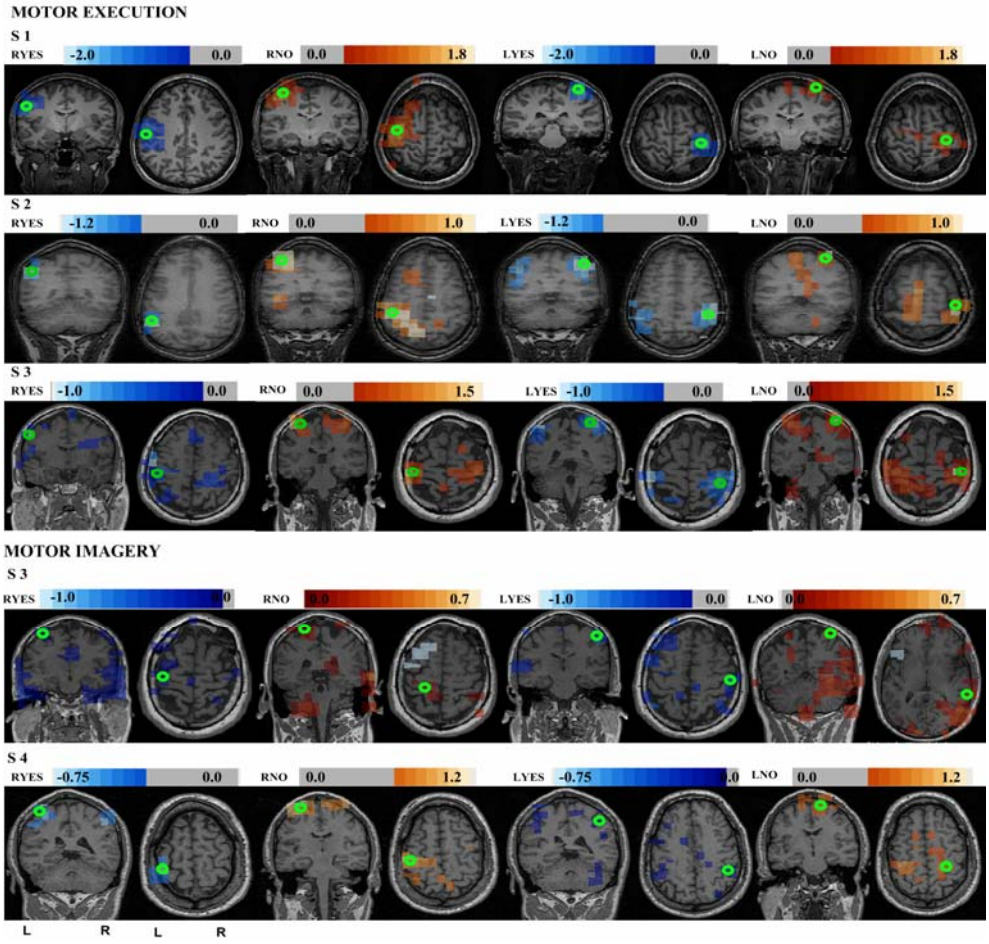

Figure 6: SAM Images for neurophysiological analysis of ERD and ERS. The Coronal and Axial view of the head is shown for Subjects 1, 2, 3 and 4. Physical movements: SAM image head plots for subject 1, subject 2 and subject 3 are given. Activation period: 0 s to 1 s after RESPONSE cue, i.e. 2.5 s – 3.5 s (see fig 3). Control period: -1 s to 0 s before the cue of RYES, LYES, RNO and LNO. Imaginary movements: SAM image head plots for subject 3 and subject 4 are given. Activation period: 1 s delay, i.e. (3 s – 4s; see fig. 3). Control period: -1 s to 0 s before the cue of RYES, LYES, RNO and LNO. Band-width: 15 - 30 Hz (Beta rhythm); Data from the activation and control windows were used for SAM analysis. The threshold bar for power in ERD/ERS for corresponding movement activity is given above each head plot. Virtual channels corresponding to ERD (blue)/ERS (red) of contra-lateral motor area activation due to movement intentions were selected from areas marked (by green circle) for further classification.

3.2. Time-Frequency Analysis in Sensor Domain

Time-Frequency analysis was performed on the single trial MEG sensor-channel data to observe the beta band ERD/ERS patterns over these channels, for each event RYES, LYES/RNO, LNO respectively. The MEG channels constrained to the central MEG sensors associated with the motor cortex area were used for the analysis. These central MEG sensors covered both the right and the left motor cortex area. The power analysis of single trial MEG sensor (from right or left motor cortex area depending on the events) signal for the active state time period with respect to beta band frequency can be seen in Fig. 7. When an MEG sensor-channel selected from the left motor cortex area was analyzed for the event RNO with the active state period for that event between the frequency band of 15 - 30 Hz, a strong, distinguishable ERS pattern was observed for almost all the subjects. Similar was the case for event LNO, for which the MEG sensor was selected from the right motor cortex area. When an MEG sensor-channel selected from the left motor cortex area was analyzed for the event RYES with the active state period for that event between the frequency band of 15-30 Hz, a distinguishable ERD pattern was observed for almost all the subjects.

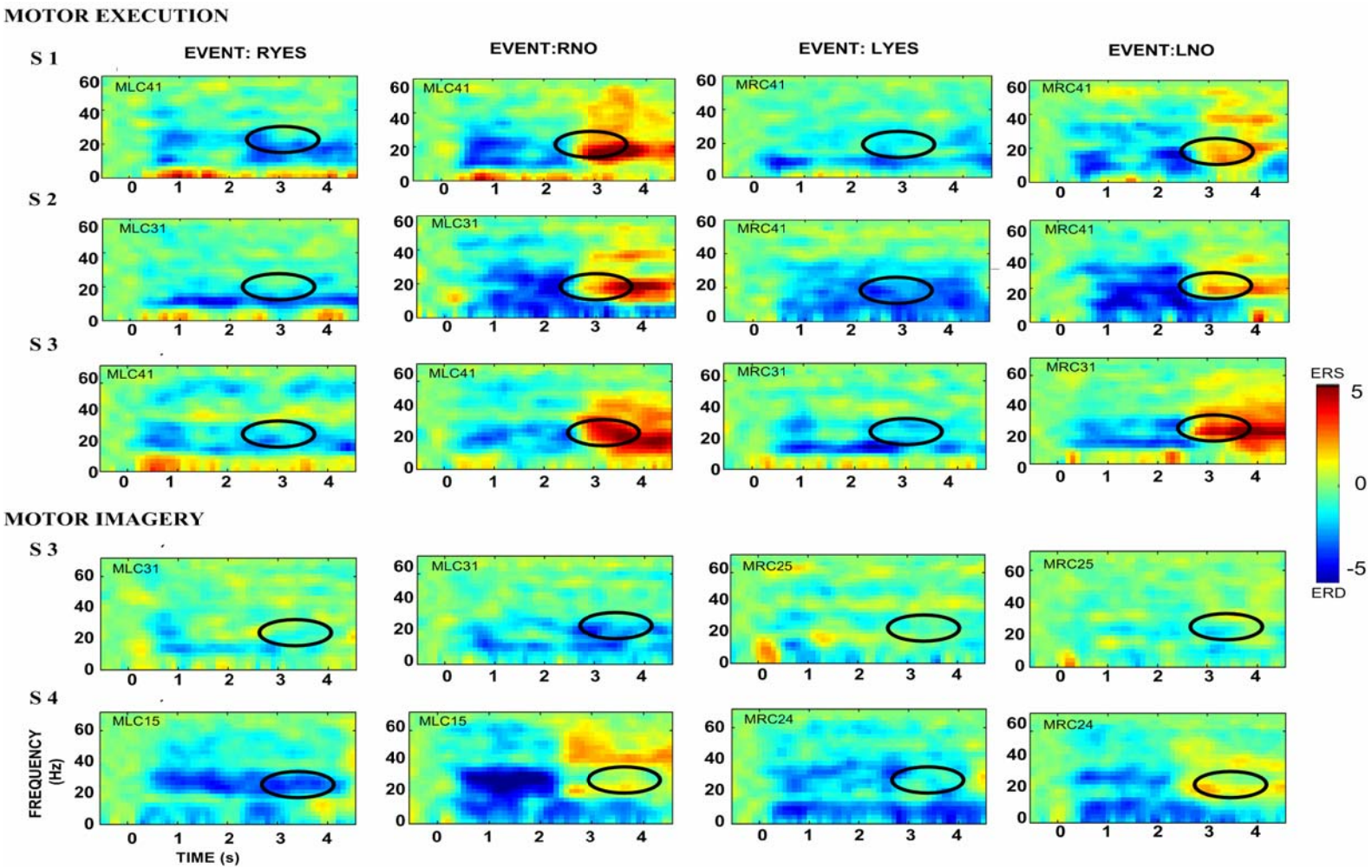

Figure 7: Time-Frequency Analysis in Sensor Domain

Time-frequency maps for events RYES, LYES, RNO and LNO for the single-trial MEG data for subjects S1, S2. S3 and S4 are plotted for corresponding MEG sensor channels (left corner of each map, M-MEG, R- Right, L-Left, and C- Central) are plotted according to hemispheric asymmetry. The power is symbolized by blue for ERD and red for ERS. The region of interest i.e. the active state period corresponding to motor execution (2.5 s – 3.5 s) and motor imagery (3 s – 4 s) showing ERD for events RYES, LYES and ERS for events RNO and LNO, is marked by the black ellipse.

Same was the case with event LYES, for which the MEG sensor-channel was selected from the right motor cortex area. It was interesting to see that, in all the subjects, ERS was more enhanced than the ERD pattern. This went with the results of a previous study which stated that ERS, the beta rebound is easier detectable in single trials than beta ERD (Pfurtscheller and Solis-Escalante 2009). The power analysis showed very weak ERD/ERS patterns for motor imagery in subject 3 (see Fig. 7) and subject 7. The delay in response to visual cues during motor imagery was again established from this power analysis and can be seen in Fig. 7.

3.3. Event-related Power Analysis for Virtual channel data

The source signals obtained from the virtual channels were used for power analysis with respect to time. As described earlier, event related power analysis was mainly performed to verify whether, ERD was a dominant pattern for virtual channels selected from the sustaining movement related events (RYES, LYES) and ERS was dominant for virtual channels selected from the ceasing of movement related events (RNO, LNO). This was done for both motor execution and motor imagery. Fig. 8 shows the power analysis of virtual channels corresponding to specific events obtained from the single trial MEG data. When the source signal from a virtual channel for the event RNO was plotted with respect to all other events (RYES, LYES, and LNO), a strong ERS was observed for the active state period for that event. Same was the case for event LNO with respect to events RYES, LYES and RNO.

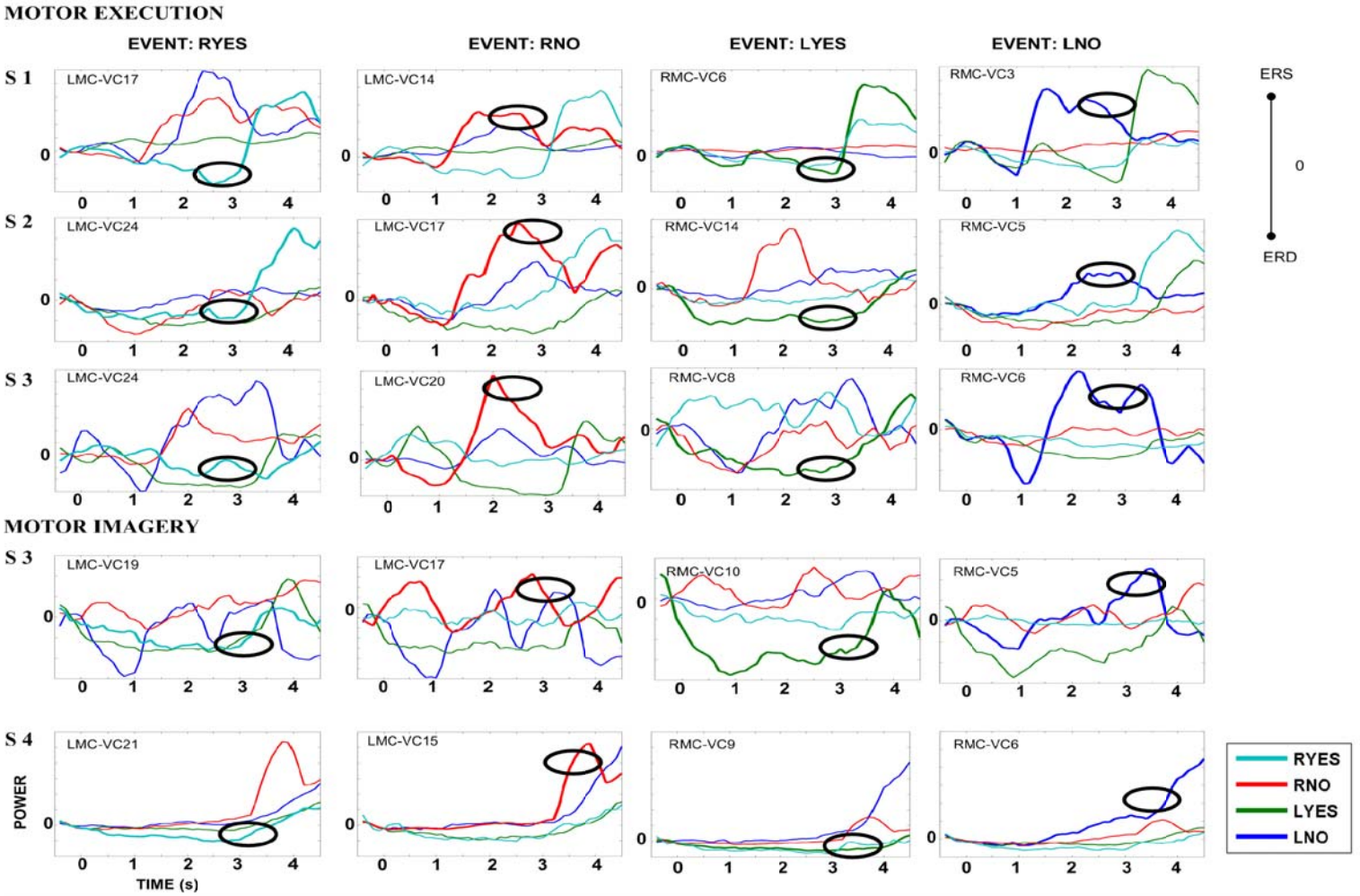

Figure 8: Time-course of Event-related Power Analysis for SAM-Virtual channel signal.

Time-power maps for events RYES, LYES, RNO and LNO for the single-trial MEG data for subjects S1, S2. S3 and S4 are plotted for corresponding SAM virtual channels (left corner of each map, RMC- Right motor cortex, LMC- Left motor cortex, VC- Virtual Channel) according to hemispheric asymmetry. The region of interest i.e. the corresponding ERD/ERS pattern is marked by the black ellipse during the active state period for motor execution (2.5 s – 3.5 s) and motor imagery (3 s – 4 s) of each event (RYES, LYES/ RNO, LNO). Legend and the power scale are provided on the right corner of the figure.

Similarly, when the source signal from a virtual channel for the event RYES was plotted with respect to all other events (LYES, RNO, and LNO), ERD was observed as a distinguishable pattern for the active state period for that event. This was also seen for the event LYES with respect to events RYES, RNO, and LNO for its active state period. The trend observed, as also seen in Fig. 8, was that the events featuring ERS were better distinguishable than the events featuring ERD.

3.4. Classification

The proposed BCI intended to discriminate four events (RYES, RNO, LYES and LNO); while sustaining and ceasing movement for the motor execution and motor imagery tasks from single trial MEG virtual channel signals obtained through SAM analysis. To verify the effectiveness of SAM, the results of SAM-Virtual channel classification were compared to MEG-Sensor based classification. Classification was carried out using GA-MLD and DTC techniques described in the methods section. The results for motor execution and motor imagery are displayed in Table 1 and Table 2 respectively.

Table 1: SAM-Virtual channel signal vs. MEG-Sensor signal for Motor Execution (ME)

Subject	SAM Virtual Sensor		MEG Sensor Domain		Total no. of samples/ trials
	GA-MLD (%)	DTC (%)	GA-MLD (%)	DTC (%)	
S 1	98.88 ± 0.71	97.38 ± 1.50	63.90 ± 4.46	53.50 ± 4.03	120
S 2	96.33 ± 1.05	87.25 ± 3.81	71.10 ± 2.28	62.50 ± 2.92	120
S 3	98.44 ± 1.09	98.44 ± 0.78	72.56 ± 2.46	67.11 ± 3.28	115
S 4	92.38 ± 1.20	85.63 ± 3.50	70.00 ± 4.22	58.11 ± 4.89	120
S 5	95.25 ± 1.54	92.75 ± 1.65	71.50 ± 3.75	55.60 ± 2.80	118
S 6	97.75 ± 1.42	98.25 ± 1.21	65.40 ± 3.90	51.80 ± 5.20	89
Average	96.51 ± 2.43	93.28 ± 5.71	69.08 ± 3.58	58.10 ± 5.79	114

Table 2: SAM-Virtual channel signal vs. MEG-Sensor signal for Motor Imagery (MI)

Subject	SAM Virtual Sensor		MEG Sensor Domain		Total no. of samples/ trials
	GA-MLD (%)	DTC (%)	GA-MLD (%)	DTC (%)	
S 3	94.63 ± 1.87	82.88 ± 2.95	39.20 ± 2.10	31.5 ± 3.34	116
S 4	88.25 ± 2.78	71.75 ± 2.65	56.40 ± 3.47	48.20 ± 2.57	120
S 5	87.25 ± 2.75	76.50 ± 2.93	59.82 ± 2.38	54.27 ± 2.43	87
S 7	88.63 ± 1.71	69.87 ± 3.51	38.33 ± 2.93	28.78 ± 3.80	114
Average	89.69 ± 3.34	75.25 ± 5.80	48.43 ± 11.26	40.68 ±12.48	110

From the results, it is clear that SAM-Virtual Channels were successful in classifying the four events at high performance. The Virtual Channel-based classification accuracy for motor execution using GA-MLD was averaged to be 96.51 % with standard deviation of 2.43 % and for motor imagery, the results for GA-MLD classification was averaged to be 89.69 % with standard deviation of 3.34 %. Similarly, the SAM-Virtual channel based classification accuracy for motor execution using direct DTC was averaged to be 93.28 % with standard deviation of 5.71 % and for motor imagery, the results for direct DTC classification was averaged to be 75.25 % with standard deviation of 5.80 %.

The MEG-Sensor based classification was performed in order to compare its results with SAM-Virtual channels. The MEG-Sensor based classification accuracy for motor execution using GA-MLD was averaged to be 69.08 % with standard deviation of 3.58 % and, for motor imagery, the results for GA-MLD was averaged to be 48.43 % with standard deviation of 11.26%. Similarly, the SAM-Virtual channel classification accuracy using direct DTC, for motor execution was averaged to be 58.10 % with standard deviation of 5.79 % and, for motor imagery, the result was averaged to be 40.68 % with standard deviation of 12.48 %. For motor imagery tasks, the classification accuracy for subjects S 3 and S 7 were found to be relatively low. It was observed by time-frequency analysis in the sensor domain, that ERS and ERD both were very weak for these subjects. ERD was hardly detected. Hence feature extraction and classification was difficult for these subjects.

3.5. Statistical Analysis

To study the statistical significance of the results established through classification accuracies between SAM and Sensor domains, a statistical analysis was done on the results obtained through GA-MLD classification technique. The significance level was chosen to be 0.05. It was of interest to know the statistical claim on two points, the first being; whether the classification accuracy obtained from SAM-Virtual channel analysis was better than that obtained through Sensor-based classification for motor execution. The second point was to determine whether the classification accuracy obtained from SAM-Virtual channel analysis was better than that obtained through sensor-based classification for motor imagery.

Using a paired *t*-test, there was clear evidence for increased classification accuracy ($t = 13.3$, $df = 5$, p-value < 0.0001) through SAM-filtered virtual channel analysis for motor execution. There was a significant improvement in the accuracy to classify the events RYES, RNO, LYES and LNO through this analysis (point estimate of +27.43%; 95% confidence interval between 22.13% and 32.73%) as compared to the sensor domain results.

For motor imagery, a paired *t*-test was again conducted and a statistically significant increase in classification accuracy ($t = 6.03$, $df = 3$, p-value < 0.0046) through SAM-filtered virtual channel analysis was observed. When compared with sensor-based classification, a significant improvement in classification of events RYES, RNO, LYES

and LNO was seen with SAM- filtered virtual channel based classification (point estimate of +41.25%; 95% confidence interval between 19.47% and 63.04%).

CHAPTER 4

Discussion

4.1. ERD/ERS Analysis for human natural motor behavior vs. motor imagery

The analysis of movement related activities was made extremely convenient due to the unique paradigm used. The asymmetric hemispheric activity during motor tasks as well as the features of ERD and ERS seen while sustaining and ceasing natural upper limb movements explicitly helped in enhancing classification accuracy. The spatial distribution of post movement beta rebound corresponding to ERS was seen to be more focal than ERD distribution. The observation that the detection of ERS might be potentially more reliable than ERD detection was used to reliably classify the four natural right and left hand motor tasks. Using natural motor behavior for the paradigm was easier and motivating for the subjects to perform both motor execution and motor imagery tasks thus minimizing training period and consequently fatigue which are a common issue during data collection. In a study conducted by Dr. Birbaumer's group, the performance of the MEG-based BCI (Mellinger et al. 2007) was similar to what had been reported for a state-of-the-art EEG-based mu rhythm BCI with a large number of participants (Guger et al. 2003). The MEG-based BCI used voluntary amplitude modulation of sensorimotor mu and beta rhythms.

The results of the present study indicate that the use of natural motor behavior for the proposed SAM-Virtual channels based BCI gives higher classification results when compared to its EEG counterpart using amplitude modulation of sensorimotor rhythms.

For SAM analysis, the ERD pattern was seen during the planning and execution of movements whereas the ERS pattern was seen after movement for all the subjects. This has been demonstrated in previous studies (Pfurtscheller 1988; Toro et al. 1994; Bai et al. 2005) . The classification accuracy results for motor execution were observed to be better than motor imagery. Studies show that the performance of motor imagery was associated with the ERD and ERS in the beta band similar to that of motor execution (Pfurtscheller et al. 2005).

It has also been reported that only the left sensorimotor cortex is activated during dominant right hand movement, whereas sensorimotor cortices of both right and left hemispheres are activated during non-dominant left hand movement. This also has been reported previously with EEG studies (Kawashima et al. 1993; Volkmann et al. 1998; Jung et al. 2003). However for the present study, during motor imagery this pattern was not always observed. Although a bilateral ERD was seen for most subjects mentioned in previous studies as the "spill over" of cortical activation (Dhamala et al. 2003), bilateral ERS was observed for subject S3 and S4 for motor imagery (See Fig. 6, Pg. 33). There was a variation of bilateral ERS in subject S3 and midline ERS in subject S2 for motor execution (See Fig. 6, Pg. 33). This could result to a lower classification accuracy due to poor feature detection, although the ERS pattern was found to be stronger in the left motor cortex area for RNO and right motor cortex area for LNO. The virtual channels for feature

selection and classification were thus selected from the dominant lobe. Since natural motor behavior i.e. right and left physical hand movement, was used for the motor execution tasks, the ERD/ERS patterns were strong and well defined. However, the ERD/ ERS patterns for motor imagery were more bilateral and were observed to be weak as compared to motor execution. Hence the feature extraction and classification of virtual channel data was difficult for motor imagery which led to lower classification accuracy for the events RYES, RNO, LYES and LNO. This can be explained by the fact that the subjects need more control over their movement intentions to achieve accuracy for motor imagery tasks. It can be achieved through more effort and longer training periods. Considering the fact that the subjects who participated in this study were naïve to BCI and this was a single trial study, more accurate motor imagery classification could potentially be obtained through a short BCI training period.

4.2. SAM-Virtual channel signal

The neurophysiological mechanisms for voluntary movement have been extensively studied with EEG and also with MEG (Vaughan et al. 1968; Deecke et al. 1969; Pfurtscheller and Berghold 1989b; Taniguchi et al. 2000; Bai et al. 2005; Bai et al. 2008) . MEG has the advantage of superior spatial resolution and can identify the anatomical location of cortical activity with enhanced accuracy. Sensor-based processing is a basic method which only minimally uses the source localization ability of MEG for further classification of event related voluntary movements. A couple of MEG studies have

been conducted based on sensor domain, focusing mainly on the source identification problems (Lee et al. 2003; Barbati et al. 2006; Kauhanen et al. 2006). SAM, when compared to Sensor-based processing, is a spatially selective beamformer, which filters out the background brain noise from other brain regions to obtain meaningful signals from the arbitrary target regions. SAM transforms neuromagnetic signals into units of dipole moment on a per-voxel basis; this enables one to display simultaneously active multiple sources, provided that these sources are not perfectly synchronized (Taniguchi et al. 2000). For the present study, further application of statistical imaging technique was applied to obtain statistical difference in the power of the selected beta frequency band which was evaluated between the active and the control states for events RYES, RNO, LYES and LNO. Those areas with statistical difference were displayed on the individual MRI (See Fig. 6, Pg. 33) in a tomographic manner (Ishii et al. 1999). Virtual channels were selected from these images. Thus SAM based virtual channels immensely facilitates feature reduction while selecting the features from the cortical areas, from the source of activation. This is a very important factor for the design of the proposed BCI because SAM-filtered virtual channels tremendously improve the signal-to-noise ratio (SNR) of the MEG signals and also reduces the computational load. In the present study, the original data from 275 MEG sensors for each subject was reduced to mere 25-30 virtual channels, with high SNR from SAM-filtered virtual channel analysis. Classification of these reliable features related to the sustaining and ceasing voluntary movements RYES, LYES, RNO and LNO, while analyzing single-trial MEG signals thus facilitates a high-performance, high-speed BCI.

4.3. Event-related Power Analysis for Virtual channels and MEG-Sensors

From the power analysis in the SAM domain, it is evident that among the four events for each virtual channel selected, the events featured by ERS were better detected for the single trial MEG signals than those featured by ERD, during the active state period. From Fig. 8, this phenomenon is clearly observed for Subjects S1, S2, and S3 for motor execution RNO and LNO events. For motor imagery, Subject S3 and subject S4 also demonstrate this phenomenon. The same can be observed in Fig.7, from power analysis in the MEG-Sensor domain. Studies have reported this phenomenon previously (Pfurtscheller and Solis-Escalante 2009). Variability in this phenomenon was seen in the MEG-Sensor domain in Subject S3, for whom ERS was not detected during the active state period in the beta band for the respective events for motor imagery trial. This suggests that, since the power samples for feature selection are calculated using the active state time window and ERS was not distinguishable for the events RNO and LNO during this period, the classification accuracy for subject S3 was low. This was the case with subject S 7 for the motor imagery trial in the sensor domain (See Table 2, Pg. 39). For Virtual channel analysis, since SAM further enhances the spatial resolution for the detection of both ERD and ERS, the selection of these features to classify the four events RYES, RNO, LYES and LNO proved highly efficient to achieve the proposed high performance BCI.

Our aim for the present study was to verify the effectiveness of SAM-filtered virtual channel signals to classify natural human movement intentions. The performance of GA-MLD classifier was observed to be better than DTC and hence GA-MLD based

classification was used for the statistical analysis to compare SAM-filtered virtual channel signal vs. the MEG-sensor signals.

4.4. Implications for BCI Application

According to the statistical analysis performed on this study, the four events RYES, LYES, RNO and LNO associated with sustained and ceased natural human motor control were efficiently classified with high accuracy by the SAM-filtered, single trial MEG based BCI. The results for GA-MLD based classification were averaged to be 96.51 % with standard deviation of 2.43 %. The results for motor execution can be immensely advantageous for disabled motor disorder patients, even with very limited physical limb movement.

For motor imagery, the results for GA-MLD classification were averaged to be 89.69 % with standard deviation of 3.34 %. Once the basic mechanism of converting event related movement intensions to computerized action is perfected, the potential uses for this BCI technology are almost limitless. This can be easily achieved through introduction of a short training session for motor imagery trial for the proposed BCI. Thus, the proposed SAM-filtered single trial MEG based BCI may help tremendously in accelerating rehabilitation and provide a means for assistive device control or communication for patients with severe movement disorders.

The whole process of SAM analysis in this study was offline. For real-time use, a calibration study may be performed to determine the source locations of the desired region

of interest. Using this model, the spatio-temporal activities of neural sources, i.e., virtual channels signal, can be estimated online. Future study is required to explore the robustness of online estimation of neural source activities from pre-determined source locations.

Due to the high costs and lack of portability, MEG is a less practical modality for BCI use compared with EEG. However the advantages of MEG include high spatial and temporal resolution and moreover the ability to use SAM for the selection of virtual channels, which further enhances the source-signal to noise ratio of MEG signals and also reduces the computational load for analyses. As technology progresses, there may be portable MEG devices, voiding the importance of shielded rooms for recording (see e.g. BabySquid, Tristan Technologies). Even though real-time processing may be difficult at present with the proposed BCI, it can be used effectively for training and rehabilitation of patients with movement disorders to improve the neural plasticity of their brain. Overall, this BCI has the following advantages over other BCIs: a natural control scheme, high spatial resolution, acceptable response time, robustness and reliability. The proposed BCI could bring improvement to the quality of life of the patients suffering from various movement disorders.

Literature Cited

Literature Cited

Andres FG, Gerloff C (1999) Coherence of sequential movements and motor learning. J Clin Neurophysiol 16: 520-527

Babiloni F, Bianchi L, Semeraro F, Millan J, Mourinyo J (2001) Mahalanobis distance-based classifiers are able to recognize EEG patterns by using few EEG electrodes. Conf Proc IEEE Eng Med Biol Soc 2001: 651-654

Bai O, Lin P, Vorbach S, Floeter MK, Hattori N, Hallett M (2008) A high performance sensorimotor beta rhythm-based brain-computer interface associated with human natural motor behavior. J Neural Eng 5: 24-35

Bai O, Lin P, Vorbach S, Li J, Furlani S, Hallett M (2007) Exploration of computational methods for classification of movement intention during human voluntary movement from single trial EEG. Clin Neurophysiol 118: 2637-2655

Bai O, Mari Z, Vorbach S, Hallett M (2005) Asymmetric spatiotemporal patterns of event-related desynchronization preceding voluntary sequential finger movements: a high-resolution EEG study. Clin Neurophysiol 116: 1213-1221

Barbati G, Sigismondi R, Zappasodi F, Porcaro C, Graziadio S, Valente G, Balsi M, Rossini PM, Tecchio F (2006) Functional source separation from magnetoencephalographic signals. Hum Brain Mapp 27: 925-934

Capon J (1969) High-Resolution Frequency-Wavenumber Spectrum Analysis. Proceedings of the Ieee 57: 1408-&

Carpenter MB (1985) Core Text of Neuroanatomy.

Deecke L, Scheid P, Kornhuber HH (1969) Distribution of readiness potential, pre-motion positivity, and motor potential of the human cerebral cortex preceding voluntary finger movements. Exp Brain Res 7: 158-168

Dhamala M, Pagnoni G, Wiesenfeld K, Zink CF, Martin M, Berns GS (2003) Neural correlates of the complexity of rhythmic finger tapping. Neuroimage 20: 918-926

Duda RO, Hart PE, Stork DG (2001) Pattern Classification. John Wiley, New York:

Garrett D, Peterson DA, Anderson CW, Thaut MH (2003) Comparison of linear, nonlinear, and feature selection methods for EEG signal classification. IEEE Trans Neural Syst Rehabil Eng 11: 141-144

Guger C, Edlinger G, Harkam W, Niedermayer I, Pfurtscheller G (2003) How many people are able to operate an EEG-based brain-computer interface (BCI)? IEEE Trans Neural Syst Rehabil Eng 11: 145-147

Hillebrand A, Singh KD, Holliday IE, Furlong PL, Barnes GR (2005) A new approach to neuroimaging with magnetoencephalography. Hum Brain Mapp 25: 199-211

Hung CI, Lee PL, Wu YT, Chen LF, Yeh TC, Hsieh JC (2005) Recognition of motor imagery electroencephalography using independent component analysis and machine classifiers. Ann Biomed Eng 33: 1053-1070

Ishii R, Shinosaki K, Ukai S, Inouye T, Ishihara T, Yoshimine T, Hirabuki N, Asada H, Kihara T, Robinson SE, Takeda M (1999) Medial prefrontal cortex generates frontal midline theta rhythm. Neuroreport 10: 675-679

Josephson BD (1974) The discovery of tunnelling supercurrents. Reviews of Modern Physics 46: 251

Jung P, Baumgartner U, Bauermann T, Magerl W, Gawehn J, Stoeter P, Treede RD (2003) Asymmetry in the human primary somatosensory cortex and handedness. Neuroimage 19: 913-923

Kauhanen L, Nykopp T, Sams M (2006) Classification of single MEG trials related to left and right index finger movements. Clinical Neurophysiology 117: 430-439

Kawashima R, Yamada K, Kinomura S, Yamaguchi T, Matsui H, Yoshioka S, Fukuda H (1993) Regional cerebral blood flow changes of cortical motor areas and prefrontal areas in humans related to ipsilateral and contralateral hand movement. Brain Res 623: 33-40

Keefer EW, Botterman BR, Romero MI, Rossi AF, Gross GW (2008) Carbon nanotube coating improves neuronal recordings. Nat Nanotechnol 3: 434-439

Laconte SM, Peltier SJ, Hu XP (2006) Real-time fMRI using brain-state classification. Hum Brain Mapp

Lee P-L, Wu Y-T, Chen L-F, Chen Y-S, Cheng C-M, Yeh T-C, Ho L-T, Chang M-S, Hsieh J-C (2003) ICA-based spatiotemporal approach for single-trial analysis of postmovement MEG beta synchronization[small star, filled]. NeuroImage 20: 2010-2030

Li J, Yao J, Summers RM, Petrick N, T. MM, Hara AT (2006) An efficient feature selection algorithm for computer-aided polyp detection. International Journal on Artificial Intelligence Tools 15: 893-915

Marques JP (2001) Pattern recognition: concepts, methods and applications. Springer-Verlag, Berlin

Mellinger J, Schalk G, Braun C, Preissl H, Rosenstiel W, Birbaumer N, Kubler A (2007) An MEG-based brain-computer interface (BCI). Neuroimage 36: 581-593

Nakaya Y, Mori H (1992) Magnetocardiography. Clin Phys Physiol Meas 13: 191-229

Oldfield RC (1971) The assessment and analysis of handedness: the Edinburgh inventory. Neuropsychologia 9: 97-113

Partridge LD (1993) The Nervous System,Its Function and Its Interaction with the World. A Bradford Book, Cambridge.

Pfurtscheller G (1988) Mapping of event-related desynchronization and type of derivation. Electroencephalogr Clin Neurophysiol 70: 190-193

Pfurtscheller G, Berghold A (1989a) Patterns of Cortical Activation During Planning of Voluntary Movement. Electroencephalography and Clinical Neurophysiology 72: 250-258

Pfurtscheller G, Berghold A (1989b) Patterns of cortical activation during planning of voluntary movement. Electroencephalogr Clin Neurophysiol 72: 250-258

Pfurtscheller G, Lopes da Silva FH (1999) Event-related EEG/MEG synchronization and desynchronization: basic principles. Clin Neurophysiol 110: 1842-1857

Pfurtscheller G, Solis-Escalante T (2009) Could the beta rebound in the EEG be suitable to realize a "brain switch"? Clin Neurophysiol 120: 24-29

Pfurtscheller J, Rupp R, Muller GR, Fabsits E, Korisek G, Gerner HJ, Pfurtscheller G (2005) [Functional electrical stimulation instead of surgery? Improvement of grasping function with FES in a patient with C5 tetraplegia]. Unfallchirurg 108: 587-590

Raymer ML, Punch WF, Goodman ED, Kuhn LA, Jain AK (2000) Dimensionality reduction using genetic algorithms. Evolutionary Computation, IEEE Transactions on 4: 164-171

Robinson SE (1998) Method for functional brain imaging from magnetoencephalographic data by estimation of source signal-to-noise ratio. U.S. Patent Application 09/138, 826 filed August 124,1998

Robinson SE (2004) Localization of event-related activity by SAM(erf). Neurol Clin Neurophysiol 2004: 109

Salmelin R, Hamalainen M, Kajola M, Hari R (1995) Functional segregation of movement-related rhythmic activity in the human brain. Neuroimage 2: 237-243

Sarvas J (1987) Basic mathematical and electromagnetic concepts of the biomagnetic inverse problem. Phys Med Biol 32: 11-22

Taniguchi M, Kato A, Fujita N, Hirata M, Tanaka H, Kihara T, Ninomiya H, Hirabuki N, Nakamura H, Robinson SE, Cheyne D, Yoshimine T (2000) Movement-related desynchronization of the cerebral cortex studied with spatially filtered magnetoencephalography. Neuroimage 12: 298-306

Toro C, Deuschl G, Thatcher R, Sato S, Kufta C, Hallett M (1994) Event-related desynchronization and movement-related cortical potentials on the ECoG and EEG. Electroencephalogr Clin Neurophysiol 93: 380-389

Vaughan HG, Jr., Costa LD, Ritter W (1968) Topography of the human motor potential. Electroencephalogr Clin Neurophysiol 25: 1-10

Vieth J, Kober H, Grummich P, Pongratz H, Ulbricht D, Brigel C, Daun A (1995) Biomagnetism: Fundamental Research and Clinical Applications. Elsevier Science, Amsterdam/New York.

Volkmann J, Schnitzler A, Witte OW, Freund H (1998) Handedness and asymmetry of hand representation in human motor cortex. J Neurophysiol 79: 2149-2154

Vrba J, Robinson SE (2001) Signal processing in magnetoencephalography. Methods 25: 249-271

Welch PD (1967) The Use of Fast Fourier Transform for the Estimation of Power Spectra: A Method Based on Time Averaging Over Short, Modified Periodograms. IEEE Trans. Audio Electroacoust. AU-15: 70-73

Whitley D (1994) A Genetic Algorithm Tutorial. Statistics and Computing 4: 65-85

Wikswo JP, Jr. (1989) Advances in Biomagnetism. 1 - 18

Williamson SJ, Kaufman L (1981) Biomagnetism. J. Magn. Magn. Mater 22: 129 - 201

Wolpaw JR, Birbaumer N, McFarland DJ, Pfurtscheller G, Vaughan TM (2002) Brain-computer interfaces for communication and control. Clin Neurophysiol 113: 767-791

Yom-Tov E, Inbar GF (2002) Feature selection for the classification of movements from single movement-related potentials. IEEE Trans Neural Syst Rehabil Eng 10: 170-177

APPENDIX A

Feature selection and Classification:

Feature Selection:

The SAM-filtered MEG virtual channel signals provided high-dimensional features; for example, 25 virtual channels with 16 frequency bins produced 400 features. Such high-dimensional features may bias the classification model producing a low testing accuracy. A compact subset of features needs to be determined for achieving a robust classification. The subset feature selection can be determined either empirically or 'data-driven'. Because of the high dependence among features, the empirical approach usually does not provide a good solution. The exhaustive search method is one of the optimal feature selection methods, which evaluates all possible subsets to determine the best subsets. For example, the exhaustive search of a subset of 3 features from 400 features results in more than ten million combinations. It is impractical to perform this due to the computational burden. We adopted a sub-optimal method of genetic algorithm-based search, which is a stochastic search in the feature space guided by the idea of inheriting, at each search step, good properties of the parent subsets found in previous steps (Raymer et al. 2000). One important procedure in the genetic algorithm-based feature selection is the evaluation of feature subsets. In this study, the feature subsets were evaluated on 10-fold cross-validation accuracy using a Mahalanobis Linear Distance (MLD) classifier in order to reduce the risk of over-training (Li et al. 2006). According to the evaluation of the feature subset, a new generation was created from the best of them. By repeating this procedure, a sub-optimal feature subset for the classification was determined. In this

approach, the dimension of feature subset should be provided previously. We performed a pilot study to investigate an optimal dimension. Because of the difference in spatial and temporal filters, it was difficult to determine an optimal dimension. We proposed the strategy of grid search from 4 to 20 with step of 4 according to the finding in the pilot study. In GA approach, the population size was 20, the number of generations was 100, the crossover probability was 0.8, the mutation probability was 0.01, and the stall generation was 20.

Because of the large number of features, the convergence speed under GA was still very slow. For the purpose of faster convergence and less risk of local minima, we proposed an approach of pre-feature selection to pre-select features having larger Bhattacharyya distance between two task conditions. The Bhattacharyya distance is the square of mean difference between two task conditions divided by the variance of the samples in two task conditions (Marques 2001). The Bhattacharyya distance was calculated on each feature (univariate) in feature pool indexing the feature separability between two task conditions, which was somewhat similar to ANOVA statistic test by evaluating the volume of the pooled covariance matrix of the class relative to the separation of their means. As Bhattacharyya distance indexes the separability directly, it is preferable for feature selection with comparison of other indexing methods, for example, the Fisher Score which indexes the similarity. The features were sorted in descending order according to their Bhattacharyya distance; the first 100 features were retained for subsequent multivariate feature selection.

Classification:

We explored three statistical classification and three neural network classification approaches. For pattern recognition, the simplest classification can be achieved by finding the minimum distance to the prototypes, usually the sample means under different tasks. For example, in the case of a two-feature two-class classification problem, the discriminant boundary is a straight line perpendicular to the linking of means and passing at half distance. Because the features are not necessarily mutually uncorrelated, we adopted linear and quadratic Mahalanobis distance, which takes covariance into account (Marques 2001). 'MLD' computed a pooled covariance matrix averaged from individual covariance matrices in two task conditions so that the discriminant boundary is hyper-planes leaning along the regression.

We explored a nonlinear classification approach using neural networks. The neural network approaches provide more complicated discriminant boundaries, for example, by using polynomial functions. Theoretically, it may provide higher accuracy in classification tasks, at least in the training procedure. Successful applications in BCI development have also been reported ((Garrett et al. 2003) and (Hung et al. 2005)).

VITA

Harsha Battapady was born on June 30th, 1984 in Mumbai, India. She received her Bachelor's degree in Instrumentation Engineering from the Mumbai University in June, 2006. She then joined graduate school at Virginia Commonwealth University in Richmond, Virginia. She was a Teaching assistant in the Department of Electrical Engineering for a brief period of time. She also was a Research Assistant in the BCI & EEG lab in the Department of Biomedical Engineering. She worked on two projects 'Spatial Detection of Multiple Movement Intentions from SAM-Filtered Single-Trial MEG Signals' and 'Decoding human movement intentions to classify right hand, left hand, leg and tongue movements from single-trial MEG signal for a possible 2-D BCI' during the course of her degree. Her work was submitted to the Journal of Clinical Neurophysiology and was also presented at EMBS, 2009. Harsha received a Master's of Science degree in Biomedical Engineering in August 2009.